Journal of
Ceramic Science
and Technology

J. Ceram. Sci. Tech., **03** [01] 35-40 (2012)
DOI: 10.4416/JCST2012-00043
available online at: http://www.ceramic-science.com

Fabrication, Microstructure and Properties of Hot-Pressed Nd:YAG Ceramics

S.M. Naga[1], M. Awaad[*1], H.F. El-Maghraby[1], W.H.Eisa[2], M. Abou el Ezz[3], F. Sommer[4] and R. Gadow[4]

[1]National Research Center, Ceramics Dept., Cairo, Egypt
[2]National Research Center, Spectroscopy Dept., Cairo, Egypt
[3]Graduate School of Excellence for Advanced Manufacturing Engineering, University of Stuttgart, IFKB, Stuttgart, Germany
[4]University of Stuttgart, IFKB, Stuttgart, Germany

received November 19, 2011; received in revised form December 23, 2011; accepted January 18, 2012

Abstract

Neodymium-doped yttrium-aluminum garnet (Nd:YAG) ceramics that contained 0.025, 0.05 and 0.10 at% Nd_2O_3 additives and exhibited nearly the same optical properties as those of a single crystal were fabricated by means of the sol-gel technique and hot press sintering method. Transparent YAG and Nd:YAG ceramics are fabricated either by high-temperature vacuum sintering or post-hot isostatic pressing but not hot pressing. 0.5 mass% TEOS was used as a sintering aid. A nearly pore-free microstructure with an average grain size of 5 – 10 μm was obtained by sintering at 1700 °C. The optical transmittance of the samples was 98 % in the 532 nm wavelength.

Keywords: YAG ceramics, Nd_2O_3 addition, optical properties, microstructure

I. Introduction

Transparent polycrystalline ceramic laser materials offer numerous advantages over materials produced with the melt growth method, especially faster production cycles. Their solid solution allows the fabrication of multi-phase, highly homogeneous transition materials having the ability to near-net-shape engineer profiles and structures before sintering [1].

Yttrium aluminum garnet, $Y_3Al_5O_{12}$ (YAG), is used widely in optical applications because it has a variety of good optical properties. Thus, translucent YAG doped with rare-earth ions ceramic is a promising material for large-size solid-state lasers, because of their excellent laser performance, low cost and short manufacturing periods of time [2–4].

YAG powders can be synthesized by means of many methods, such as the solid-state reaction [5,6], coprecipitation [7–9], sol-gel [10,11], spray thermal decomposition and spark plasma sintering techniques [12,13]. Zhang *et al.* [3] synthesized YAG:Tb phosphors in a novel nitrate-citrate sol-gel combustion process. With this process, single-phase cubic YAG phosphors were prepared at temperatures as low as 800 °C.

For preparation of high-optical-quality ceramics, structurally pure and non-aggregated nano-powders are required. However, sintering usually causes grain growth to the micrometric range. There are three main methods to prevent grain growth during sintering: 1. Pressure-assisted sintering, 2. Addition of dopants to modify the diffusion process in the grain boundaries, and 3. Sintering powders in metastable crystallographic phases [14].

Nd^{3+} ions were added in small proportions to the YAG matrix to improve its luminescent properties. They enter into solid solution within the garnet crystallographic lattice where they substitute Y^{3+} ions species owing to size and electric charge criteria [15]. Nd-doped yttrium aluminum garnet (Nd:YAG) single crystals have excellent chemical stability, good optical and temperature creep resistance. Nd:YAG single crystals are widely used in medicine and various industries. The Nd:YAG transparent ceramics are considered to be an alternative to single crystal because of their excellent performance, low-cost, ease of manufacture and mass production capability [16].

The methods for fabrication of transparent YAG or Nd:YAG ceramics are either high-temperature vacuum sintering [17,18] or post-hot isostatic pressing [19–21]. It is well known that the use of sintering aids such as MgO or SiO_2 is necessary to reach fully dense and transparent Nd:YAG ceramics [12,22,23]. Sallè *et al.* [24] pointed out that small additions of silica enhance densification kinetics and inhibit abnormal grain growth at the final stage of sintering. They showed that the liquid phase formed around 1660 °K is a result of the solid-state reaction between silica and YAG particles. The chemical composition of the formed liquid phase belongs to the eutectic compound in the SiO_2-Al_2O_3-Y_2O_3 pseudo-ternary phase diagram [25]. Many studies reported the beneficial role of silica addition upon sintering by suggesting the increase of the grain

* Corresponding author: elgheetany@yahoo.com

boundary (GB) diffusion coefficient or the decrease of GB surface energy in the presence of secondary phase [12]. Stevenson *et al.* [22] have recently shown that SiO_2 addition accelerates densification as well as grain growth and that in order to limit grain size to ~ 3 μm in sinter-HIPed components, the silica content can be reduced to 0.035 wt%.

The present study throws some light on the optical and mechanical properties of hot-pressed Nd:YAG ceramics for laser applications.

II. Materials and Methods

For the preparation of YAG and Nd:YAG ceramics, chemically pure reagents of Y_2O_3 (> 99.9 %-Y, Strem chemicals, Newburyport, MA, USA), aluminum tri-isopropoxide (Merck, Germany) and Nd_2O_3 (99.9 %-Nd, Strem chemicals, Newburyport, MA, USA) were used as starting materials.

Predetermined amounts of aluminum tri-isopropoxide, yttrium oxide and neodymium oxide according to the stoichiometric formula $Nd_xY_{3-x}Al_5O_{12}$, where x=0, 0.025, 0.05 and 0.1, were carefully weighed. Aluminum alkoxide was hydrolyzed in hot distilled water under vigorous stirring for 2 h at 80 °C. The hydrolyzed aluminum alkoxide was peptized with the addition of 4 ml nitric acid, which led to a transparent sol, and was left to cool. Meanwhile, yttrium oxide was dissolved in hot diluted nitric acid. The yttrium nitrate mixture was then evaporated to almost dryness to get rid of the excess nitric acid. In case of Nd:YAG ceramics, Nd_2O_3 was treated in the same way as the yttrium oxide and the two yttrium and neodymium nitrates were then mixed together. The nitrate mixture was gently added to the boehmite sol and the concentration of the sol was adjusted at 0.5 M. The transparent sol mixture was left at room temperature till gel formation. 0.5 mass% TEOS solution was added on weight. The gel was dried at 110 °C till complete dryness and then calcined in an electric oven for 2 h at 700 °C to get rid of all organic and nitrate species. The calcined powder was ground in an automatic agate mortar and pestle to remove all particle agglomerations, and then attrition-milled for up to 2.5 h using 5-mm yttria stabilized zirconia balls and isopropyl alcohol media to d_{50} = 5.27 μm (Malvern laser master size analyzer, UK) and 1 h using 2-mm balls to d_{50} = 3.09 μm. The as-prepared and milled YAG powder was further examined with transmission electron microscopy (TEM Jeol 1230, Japan) to indicate the actual grain size of the YAG particles.

The thermal analysis of the powdered samples (before calcination) was conducted using a thermal analyser (SDT Q 600 V20.5 Build 15 USA) with a heating rate of 10 °C/min with alumina as a reference material.

The powders were hot-pressed at 1700 °C under a pressure of 60 MPa using a graphite die with an internal diameter of 45 mm, a heating rate of 50 K min^{-1} and 1 h dwell time. The discs were ground and polished to 6 μm and finally finished with 1 μm diamond paste. Microhardness testing was conducted according to DIN 50359 using Vickers indentation with 0.1 kg force and 10 s dwell time (Fischer WIN-HCU, Germany), an average of 10 readings were performed for all samples.

The phase constitutions of the fired composites were determined using an X-ray diffractometer (Philips 1730, the Netherlands) with secondary CuKα radiation and graphite monochromator. FTIR absorption spectra were measured with the KBr disc technique (Jasco 6100 spectrophotometer) in the range 400 – 4000 cm^{-1} at a resolution of ± 4 cm^{-1}. A continuous diode laser with an emission wavelength of 807 nm and pulsed laser with emission a wavelength of 532 nm were used as excitation sources for the absorbance measurements.

Careful grinding of the sample is of great importance to eliminate errors caused by scattering. The microstructure of the composites was evaluated with a scanning electron microscope (Philips XL 30, the Netherlands) with acceleration voltage of 30 kV (secondary emission), the surfaces were coated with a thin layer of gold to conduct the electric current.

III. Results and Discussion

The TEM micrograph of the as-prepared and milled YAG powder is shown in Fig. 1a. For phosphor applications, one of the requirements is the particle size distribution; uniform and ultrafine phosphors are desirable to achieve high resolution. The mean particle size was estimated to be 16 nm. The selected area diffraction pattern (Fig. 1b and Table 1) of the YAG powder clearly indicates the highly polycrystalline nature of the particles.

Table 1: ED data of YAG ($Y_3Al_5O_{12}$) powder

Phase	hkl	d values		
		JCPDS (Card no. 88 – 2047)	The present study	
			XRD	ED
YAG ($Y_3Al_5O_{12}$)	4 2 0	2.684	2.683	2.648
	4 0 0	3.000	2.999	3.030
	3 2 1	3.208	3.207	3.215
	2 2 0	4.243	4.244	4.227
	2 1 1	4.900	4.905	4.967

The thermal decomposition of the YAG precursor was studied in DTA/TG analyses as shown in Fig. 2. The total weight losses were found to be around 9 %. Most of the weight loss takes place at temperatures up to 500 °C, which can be attributed to the removal of the molecular water and decomposition of organic species in the precursor powder. The DTA curve displays an endothermic peak at about 100 °C, which is assigned to the removal of molecular water, while the broad exothermic peak at ~500 °C is due to the decomposition and oxidation of organic materials. The sharp exotherm at ~951 °C is attributed to the crystallization of YAM ($Y_4Al_2O_9$) phase. The exothermic peak at 1059 corresponds to YAP ($YAlO_3$) formation. Wen *et al.* [26] found that YAM and YAP were formed between 900 – 1100 °C and 1100 – 1250 °C respectively depending on the size of the starting powders. The Al_2O_3 polymorph present at 1000 °C is most likely θ-Al_2O_3 which usual-

ly shows low crystallinity and transforms to highly crystalline α-Al_2O_3 at ~1200 °C [27,28]. The broad exothermic peak at 1251 °C is due to the crystallization of YAG phase according to the equation [29]:

$$3YAlO_3 + Al_2O_3 \rightarrow Y_3Al_5O_{12} \quad (1)$$

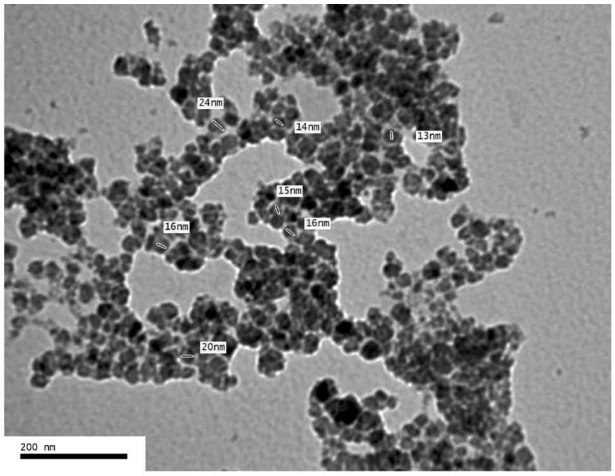

a

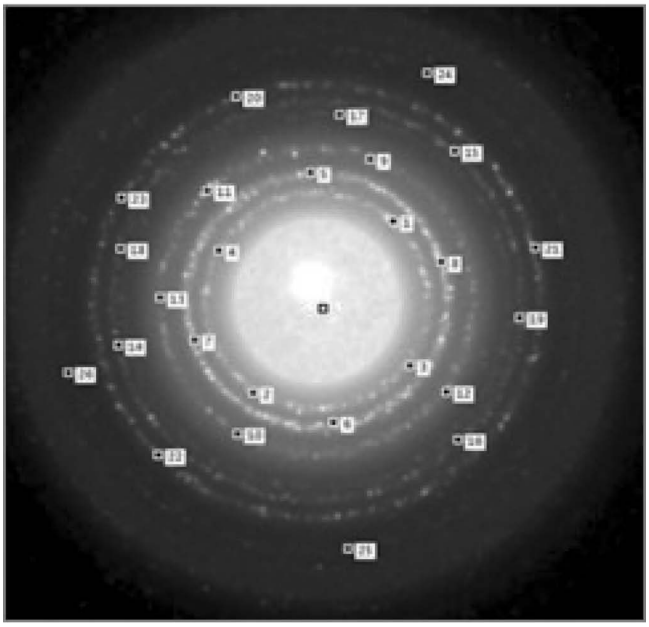

b

Fig. 1: (a) TEM micrograph of undoped YAG powder and (b) selected area electron diffraction pattern of the undoped YAG powder.

Fig. 3 shows the XRD patterns of the doped and undoped YAG hot-pressed samples. It is clear that all peaks of the samples can be well indexed as the cubic garnet structure of YAG (JCPDS: 88 – 2047). It indicates that full transformation to YAG occurred during hot pressing despite the introduction of Nd and SiO_2 additives.

The FTIR spectra of the fired YAG samples undoped and doped with different Nd at.% are listed in Table 2. The spectra exhibited well-defined peaks at 1080 – 1088 cm^{-1} and 788 – 790 cm^{-1} due to stretching vibrations of the AlO_6 octahedron. Also, it showed absorption peaks at 462 – 467 and 423 – 441 cm^{-1} associated with stretching of AlO_4 tetrahedron, while the peaks at 720, 570 and 513 cm^{-1} represent the characteristics of Y-O-Al-O vibrations. All of which matched with the reported data for a well-crystallized YAG [30–32]. New bands appeared at ~ 473 and 410 cm^{-1} in the infrared absorption spectra of the Nd-doped samples. These bands are due to the stretching vibration mode of Nd-O.

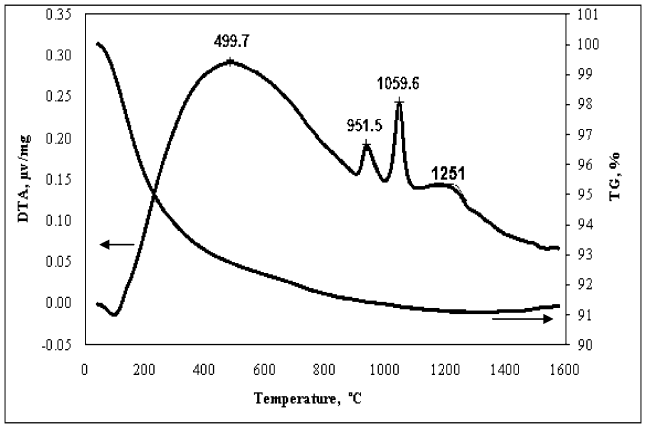

Fig. 2: DTA/TG analyses of the undoped YAG precursor

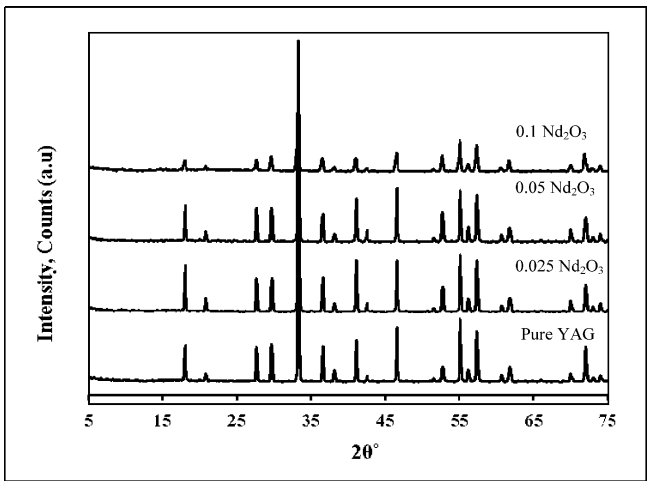

Fig. 3: XRD patterns of doped and undoped YAG powders sintered at 1700 °C for 1 h.

Figs. 4a, b and c show the fracture surfaces of Nd-doped and undoped YAG specimens. Undoped YAG exhibited a nearly pore-free structure, possibly owing to grain boundary diffusion. For the $Nd_{0.025}Y_{2.975}Al_5O_{12}$ and $Nd_{0.1}Y_{2.9}Al_5O_{12}$, quite a few pores located at the grain boundaries can be observed. In all specimens, some grain boundaries could not be detected. The well-crystallined Nd:YAG ceramics converted into pseudo-amorphous state, as attributed to the addition of sintering aid (SiO_2). On sintering, SiO_2 and the impurities introduced during processing and milling enhanced the driving force of some crystalline phase to pseudo-amorphous phase transformation. The obtained results are in agreement with those obtained by Li *et al.* [33]. The average grain sizes of the $Nd_{0.025}Y_{2.975}Al_5O_{12}$ and $Nd_{0.1}Y_{2.9}Al_5O_{12}$ are ~5 μm, which are smaller than Nd-free YAG with average grain size of ~10 μm. It seems that the grain growth mechanism of liquid-phase sintering of Si-doped Nd:YAG samples is limited by the ionic diffusion through the intergranular liquid phase. As reported in the literature for neodymium [34], the bulk diffusion coefficient of the rare-earth elements in polycrystalline YAG is about five orders of mag-

nitude smaller than grain boundary diffusion coefficient. This phenomenon could be explained as defect hosts, i.e. the zone where the formation of the segregation of cations (e.g. Al^{3+}, Y^{3+} or Nd^{3+}) vacancies could be favored [35,36]. Boulesteix *et al.*[15], showed that the grain growth kinetics during the Nd: YAG liquid-phase sintering (i.e. with silica additions) obey an Ostwald ripening mechanism. They observed that the coarsening mechanism is governed by the rare earth element or alumina cation diffusion through the liquid phase. The added silica (0.5 %) allows an improvement in the kinetic of the Nd^{3+} migration either by decreasing the average grain size of sintered YAG specimens or by leading to the appearance of a silica-enriched liquid at the grain boundary [15]. The micrographs of the specimens do not show secondary phases and no pores appear in or between the grains.

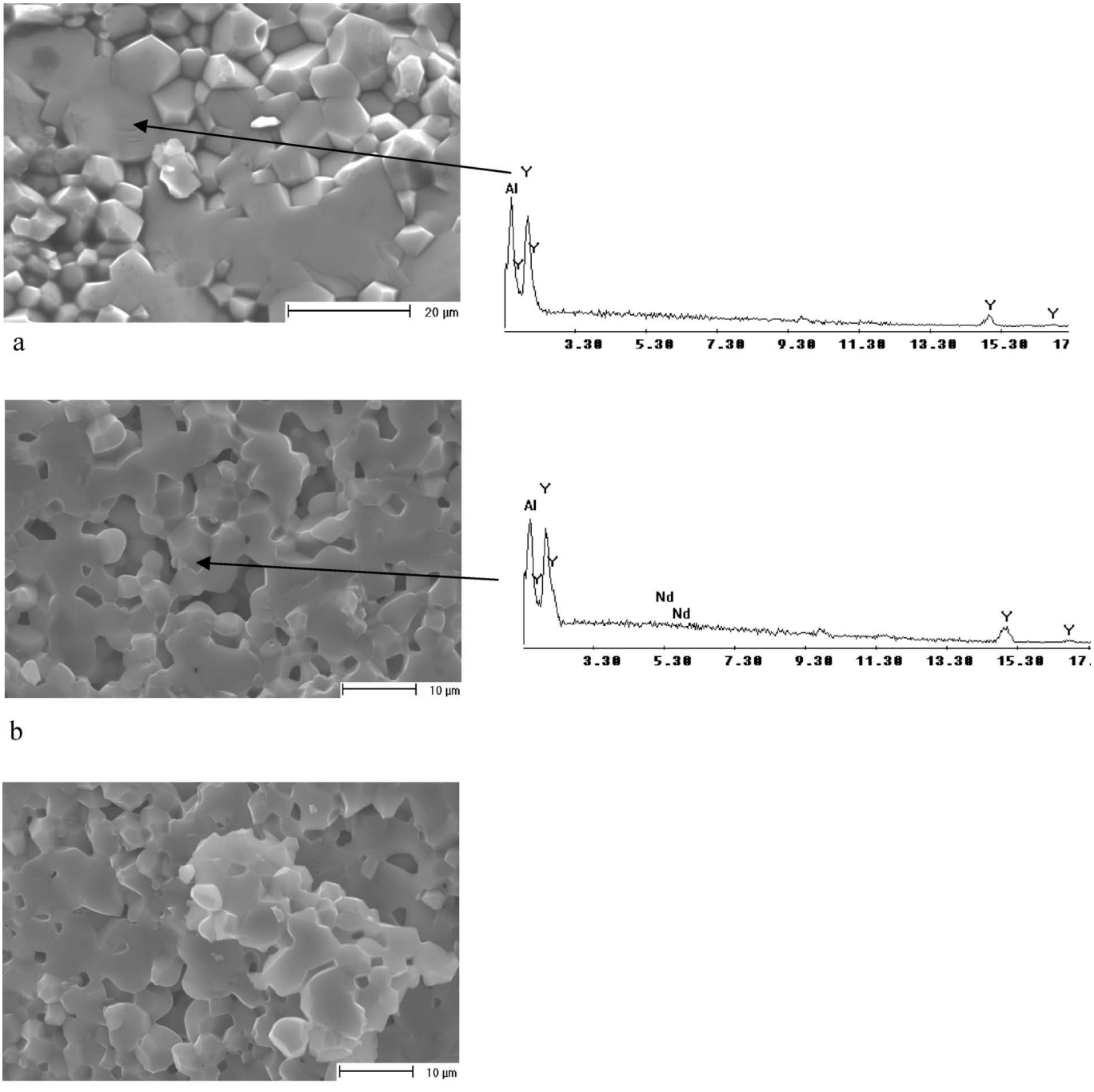

Fig. 4: SEM micrographs of (a) undoped, (b) 0.025 Nd- and (c) 0.1 Nd-doped YAG ceramics hot pressed at 1700 °C for 1 h.

Table 2: Assignments of the FTIR absorption bands of YAG ceramics

Absorption bands, cm^{-1}				Assignment
Pure YAG	$Nd_{0.1}Y_{2.9}Al_5O_{12}$	$Nd_{0.05}Y_{2.95}Al_5O_{12}$	$Nd_{0.025}Y_{2.975}Al_5O_{12}$	
1088	1088	1088	1080	Al-O st.vib.
790	788	788	790	Al-O
726	726	727	727	Y-O st. vib.
693	693	694	693	Y-O st vib.
570	568	568	569	Y-O st vib.
513	510	517	513	Y-O st vib.
–	480	473	473	Nd-O st. vib.
467	462	460	462	Al-O st.vib.
423	433	441	431	Al-O st.vib.
–	409	413	415	Nd-O st. vib.

Table 3: Studied YAG samples microhardness (HV)

Sample	Pure YAG	$Nd_{0.1}Y_{2.9}Al_5O_{12}$	$Nd_{0.05}Y_{2.95}Al_5O_{12}$	$Nd_{0.025}Y_{2.975}Al_5O_{12}$
HV	1726.00±20	1736.80±29	1795.90±25	1838.57±31

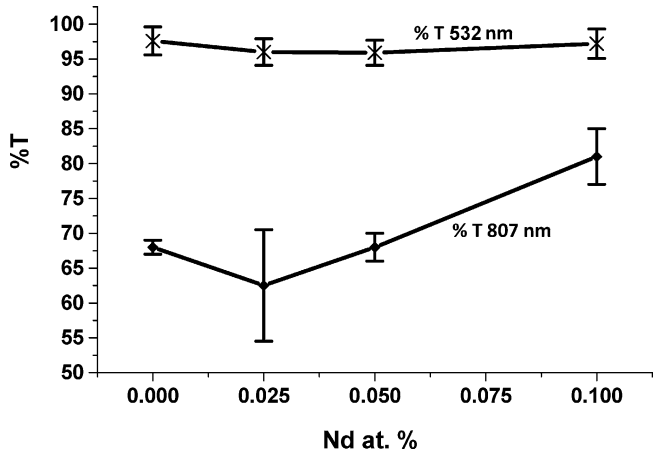

Fig. 5: The transmittance behavior of the Nd:YAG ceramic composites

The microhardness of the tested specimens is shown in Table 3. It could be seen that the value of the microhardness increased from 1726 to 1838.57 with the increase of Nd- at.%. It has been commonly accepted that the microhardness generally increases with decreasing grain size, as the dislocations generated by the indenter are blocked by the grain boundaries [37]. Light transmission is the main parameter for measuring the optical properties of transparent ceramics. The transmission behavior of the Nd:YAG ceramic samples doped and undoped with different Nd- at.% studied using CW laser diode and CW pulsed laser is shown in Fig. 5. The results showed that the transmission of the YAG and Nd:YAG samples was 97.6 % of the total power at the wavelength of 532 nm, which is even better than that of single crystal. On the other hand, transmission of continuous laser beam at wavelength of 807 nm decreased with the addition of 0.025 at% Nd_2O_3 but it increased with further increase in the Nd at.% (from about 70 % for undoped YAG samples to about 80 % for 0.10 at% doped Nd:YAG samples).

IV. Conclusions

1 Nearly pore-free Nd:YAG transparent ceramics were fabricated with the hot pressing technique at 1700 °C for 1 h.
2 Micrographs of the sample microstructures showed clean grain boundaries with no secondary phase formation either in the grain boundary or the inner grain.
3 The transmittance of the prepared Nd:YAG samples was 97.6 % at a wavelength of 532 nm (pulsed CW laser)
4 The prepared samples can be used as a beam splitter for CW lasers at a wavelength of 807 nm; 30/70 and 20/80.

Acknowledgment

The authors express their great appreciation to physicist Ayman M. Mohamed, Spectroscopy Dept., NRC, Cairo, Egypt for his assistance in the laser experiments. This work was supported by the German-Egyptian Scientific Projects (GESP) fund (Grant ID: 1388).

References

1 Taira, T.: Ceramic YAG lasers, *C.R. Phys.*, **8**, 138 – 152, (2008).
2 Zhang, J.-J., Ning, J.-W., Liu, X.-J., Pan, Y.-B., Huang, L.-P.: A novel synthesis of phase-pure ultrafine YAG: tb phosphor with different tb concentration, *Mater. Lett.*, **57**, 3077 – 3081, (2003).
3 Zhang, X., Liu, H., He, W., Wang, J., Li, X., Boughton, R.I.: Novel synthesis of YAG by solvothermal method, *J. Cryst. Growth*, **275**, e1913 – e1917, (2005).
4 Sim, S.M., Keller, K.A., Mah, T.I.: Phase transformation in yttrium aluminum garnet powders synthesized by chemical methods, *J. Mater. Sci.*, **35**, 713 – 717, (2000).

[5] Qing, L.C., Bo, Z.H., Fu, Z.M., Cai, H.J., He, M.S.: Fabrication of transparent YAG ceramics by traditional solid state reaction method, *T. Nonferr Metal Soc.*, **17**, 148 – 153, (2007).

[6] Tsai, M-S., Fu, W-C., Wu, W-C., Chen, C.-H., Yang, C-H.: Effect of aluminum source on the formation of yttrium aluminum garnet (YAG) powder via solid state reaction, *J. Alloy. Compd.,* **455**, 461 – 464, (2008).

[7] Li, X., Li, Q., Wang, J., Yang, S., Liu, H.: Synthesis of Nd3+ doped nano-crystalline yttrium aluminum garnet (YAG) powders leading to transparent ceramic, *Opt. Mater.*, **29**, 528 – 531, (2007).

[8] Saladino, M.S., Caponetti, E.: Co-precipitation synthesis of Nd:YAG nanopowders II: the effect of nd dopant addition on luminescence properties, *Opt. Mater.*, **32**, 89 – 93, (2009).

[9] Qin, X., Yang, H., Zhao, G., Luo, D., Zhang, J., Wang, S., Ma, J.: Synthesis of submicron-sized spherical Y_2O_3 powder for transparent YAG ceramics, *Mater. Res. Bull.*, **46**, 170 – 174, (2011).

[10] Fujioka, K., Saiki, T., Motokoshi, S., Fujimoto, Y., Fujita, H., Nakatsuka, M.: Pre-evaluation method for the spectroscopic properties of YAG powder, *Ceram. Int.*, **35**, 2393 – 2399, (2009).

[11] Jiao, C., Xiaogu, H., Lixi, W., Qitu, Z.: Preparation and properties of Nd:YAG ultra-fine powders, *J. Rare Earth*, **29**, 44 – 47, (2011).

[12] De, G., Van Dijk, V.A.H.: Translucent Y3Al5O12 ceramics, *Mater. Res. Bull.*, **19**, 1669 – 1674, (1984).

[13] Frage, N., Kalabukhov, S., Sverdlov, N., Ezersky, V., Dariel, M.P.: Densification of transparent yttrium aluminum garnet (YAG) by SPS processing, *J. Eur. Ceram. Soc.*, **30**, 3331 – 3337, (2010).

[14] Bowen, P., Carry, C.: From powder to sintered Pieces: forming, transformation and sintering of nanostructured ceramic oxides, *Powder Technol.*, **128**, 248 – 255, (2002).

[15] Boulesteix, R., Maître, A, Baumard, J.F., Rabinovitch, Y., Sallè, C., Weber, S., Kilo, M: The effect of silica doping on neodymium diffusion in yttrium aluminum garnet Ceramics: implications for sintering mechanism, *J. Eur. Ceram. Soc.*, **29**, 2517 – 2526, (2009).

[16] Lu, J., Prabhu, M., Xu, J., Ueda, K., Yagi, H., Yanagitani, T.: Highly efficient 2 % Nd:Yttrium aluminum garnet ceramic laser, *Appl. Phys. Lett.*, **77**, 3707 – 3709, (2000).

[17] Lee, S.G., Kochawattana, S., Messing, G.L., Dumm, J.Q., Quarbes, G., Castillo, V.: Solid-state reaction sintering of transparent polycrystalline Nd:YAG ceramics, *J. Am. Ceram. Soc.*, **89**, 1945 – 1950, (2006).

[18] Ikesue, A., Furusato, I.: Fabrication of polycrystalline transparent YAG ceramics by solid-state reaction method, *J. Am. Ceram. Soc.*, **78**, 225 – 228, (1995).

[19] Sellappan, P., Jayaram, V., Chokshi, H., Divakar, C.: Synthesis of bulk, dense, nanocrystalline yttrium aluminum garnet from amorphous powders, *J. Am. Ceram. Soc.*, **90**, 3638 – 3641, (2007).

[20] Ikesue, A., Kamata, K.: Microstructure and optical properties of hot isostatically pressed Nd:YAG ceramics, *J. Am. Ceram. Soc.*, **79**, 1927 – 1933, (1996).

[21] Lee, S.H., Kupp, E.R., Stevenson, A.J., Anderson, J.M., Messing, G.L., Li, X.: Hot isostatic pressing of transparent Nd:YAG ceramics, *J. Am. Ceram. Soc.*, **92**, 1456 – 1463, (2009).

[22] Stevenson, A.J., Li, X., Martinez, M.A., Anderson, J.M., Suchy, D.L., Kupp, E.R., Dickey, E.C., Muller, K.T., Messing, G.L.: Effect of SiO_2 on densification and microstructure development in Nd:YAG transparent ceramics, *J. Am. Ceram. Soc.*, **94**, [5], 1380 – 1387, (2011).

[23] Li, Y., Zhou, S., Lin, H., Hou, X., Li, W., Teng, T., Jia, T.: Fabrication of Nd:YAG transparent ceramics with TEOS, MgO and compound additives as sintering aids, *J. Alloys Compd.*, **502**, 225 – 230, (2010).

[24] Sallé, C., Maître, A., Baumard, J.F., Rabinovitch, Y.: A first approach of silica effect on the sintering of Nd:YAG, *Opt. Rev.*, **14**, 169 – 172, (2007).

[25] Maître, A., Sallé, C., Boulesteix, R., Baumard, J.F., Rabinovitch, Y.: Effect of silica on the reactive sintering of polycrystalline Nd:YAG ceramics, *J. Am. Ceram. Soc.*, **91**, 406 – 413, (2008).

[26] Wen, W., Sun, X., Xiu, Z., Chen, S., Tsai, C.T.: Synthesis of nanocrystalline yttria powder and fabrication of transparent YAG ceramics, *J. Eur. Ceram. Soc.*, **24**, 2681 – 2688, (2004).

[27] Hayashi, K., Toyoda, S., Takebe, H., Morinage, K.: Phase transformation of alumina derived from ammonium aluminum carbonate hydroxide (AACH), *J. Ceram. Soc.,* **99**, 550 – 555, (1991).

[28] Saraswati, V., Rao, G.V.N., Rao, G.V.R.: Structural evolution in alumina gel, *J. Mater. Sci.*, **22**, 2529 – 2534, (1987).

[29] Neiman, A.Y., Tkachenko, E.V., Kvichko, L.A., Kotok, L.A.: Conditions and mechanisms of the solid-phase synthesis of yttrium aluminates, *Russ. J. Inorg. Chem.*, **25**, 1294 – 1297, (1980).

[30] Li, J., Pan, Y.B., Qiu, F.G., Wu, Y.S., Liu, W.B., Guo, J.K.: Synthesis of nanosized Nd:YAG powders via sol gel combustion, *Ceram. Int.*, **33**, 1047 – 1052, (2007).

[31] Li, X., Liu, H., Wang, J.Y., Cui, H.M., Han, F.: Production of nano-sized YAG powder with spherical morphology and nano-aggregation via a solvothermal method, *J. Am. Ceram. Soc.*, **87**, 2288 – 2290, (2004).

[32] Panneerselvam, M., Subanna, G.N., Rao, K.J.: Translucent yttrium aluminum Garnet: microwave-assisted route to synthesis and processing, *J. Mater. Res.*, **16**, 2773 – 2776, (2001).

[33] Li, J., Wu, Y., Pan, Y., Liu, W., Huang, L., Guo, J.: Fabrication, microstructure and properties of highly transparent Nd:YAG laser ceramics, *Opt. Mater.*, **31**, 6 – 17, (2008).

[34] Yagi, H, Takaichi, K., Ueda, K.I., Yamasaki, Y., Yanagitani, T., Kamin-Skii, A.A.: The physical properties of composite YAG ceramics, *Laser Phys.*, **15** 1338 – 1344, (2005).

[35] Dieckmann, R.: Point defects and transport in non-stoichiometric Oxides: solved and unsolved problems, *J. Phys. Chem. Solids*, **59**, 507 – 525, (1998).

[36] Badrour, L., Moya, E.G., Bernodini, J., Moya, F.: Fast diffusion of silver in single and polycrystals of α-alumina, *J. Phys. Chem. Solids*, **50**, 551 – 561, (1989).

[37] McColm, I.J.: Ceramic hardness, Plenum Press, New York, 6, (1990).